The FASEB Journal • Research Communication

Retinoid receptors trigger neuritogenesis in retinal degenerations

Yanhua Lin,* Bryan W. Jones,* Aihua Liu,* James F. Tucker,* Kevin Rapp,* Ling Luo,* Wolfgang Baehr,*,†,‡ Paul S. Bernstein,* Carl B. Watt,* Jia-Hui Yang,* Marguerite V. Shaw,* and Robert E. Marc*,[1]

*Department of Ophthalmology, John A. Moran Eye Center, School of Medicine, †Department of Neurobiology and Anatomy, Health Science Center, and ‡Department of Biology, University of Utah, Salt Lake City, Utah, USA

ABSTRACT **Anomalous neuritogenesis is a hallmark of neurodegenerative disorders, including retinal degenerations, epilepsy, and Alzheimer's disease. The neuritogenesis processes result in a partial reinnervation, new circuitry, and functional changes within the deafferented retina and brain regions. Using the light-induced retinal degeneration (LIRD) mouse model, which provides a unique platform for exploring the mechanisms underlying neuritogenesis, we found that retinoid X receptors (RXRs) control neuritogenesis. LIRD rapidly triggered retinal neuron neuritogenesis and up-regulated several key elements of retinoic acid (RA) signaling, including retinoid X receptors (RXRs). Exogenous RA initiated neuritogenesis in normal adult retinas and primary retinal cultures and exacerbated it in LIRD retinas. However, LIRD-induced neuritogenesis was partly attenuated in retinol dehydrogenase knockout (*Rdh12*$^{-/-}$) mice and by aldehyde dehydrogenase inhibitors. We further found that LIRD rapidly increased the expression of glutamate receptor 2 and β Ca^{2+}/calmodulin-dependent protein kinase II (βCaMKII). Pull-down assays demonstrated interaction between βCaMKII and RXRs, suggesting that CaMKII pathway regulates the activities of RXRs. RXR antagonists completely prevented and RXR agonists were more effective than RA in inducing neuritogenesis. Thus, RXRs are in the final common path and may be therapeutic targets to attenuate retinal remodeling and facilitate global intervention methods in blinding diseases and other neurodegenerative disorders.—Lin, Y., Jones, B. W., Liu, A., Tucker, J. F., Rapp, K., Luo, L., Baehr, W., Bernstein, P. S., Watt, C. B., Yang, J.-H., Shaw, M. V., Marc, R. E. Retinoid receptors trigger neuritogenesis in retinal degenerations. *FASEB J.* 26, 81–92 (2012). www.fasebj.org**

Key Words: retinoic acid · Ca^{2+}/calmodulin-dependent protein kinase II · ionotropic glutamate receptor

Adult-onset neuritogenesis is activated in a range of central nervous system (CNS) neurodegenerative disorders, including retinal degeneration (1–5), temporal lobe epilepsy (6, 7), amyotrophic lateral sclerosis (8), Alzheimer's disease (9), and stroke (10). Most of these conditions involve an initial disruption of afferent drive followed by neural remodeling (1, 4), including neuritogenesis (11–14), the consequences of which are context dependent and may be beneficial, neutral, or detrimental (11). In retinal degenerations, such as age-related macular degeneration and retinitis pigmentosa, neuritogenesis is corruptive (4, 15) and compromises vision rescue strategies (16). Therapeutic windows for genetic, optogenetic, molecular, cellular, and bionic rescues are severely limited by bipolar cell dendrite truncation, glutamate receptor reprogramming, atypic *de novo* neuritogenesis, and rewiring (17, 18). Maximizing the outcomes of therapies for retinal degeneration and many CNS disorders requires understanding the initiators of anomalous neuritogenesis and discovery of molecular targets that may regulate corruptive network formation.

Exploring the signaling mechanisms in neurodegenerations is hampered by slow disease onset, as well as complex, episodic, and prolonged disease progressions even in well-known systems, such as mouse models of human retinitis pigmentosa (1). It is further complicated by the high diversity of neural cells. The albino rodent light-induced retinal degeneration (LIRD) model is a rapid-onset adult retinal degeneration that mimics, with temporal precision of hours, every remodeling feature of classic inherited retinal degeneration in a compressed and orderly progression, including the disruption of the choriocapillaris-retinal pigmented epithelium (RPE) barrier in age-related macular degeneration (AMD) (19). Analysis of neuritogenesis in retina is also facilitated by the abundance of retinal cell-specific markers and its precise lamination.

While many candidate mechanisms for neuritogenesis exist, it appears that key CNS development programs are accessible in mature brain to mediate plas-

[1] Correspondence: Department of Ophthalmology, John A. Moran Eye Center, 65 Mario Capecchi Dr., University of Utah, Salt Lake City, UT 84132, USA. E-mail: robert.marc@hsc.utah.edu

doi: 10.1096/fj.11-192914

This article includes supplemental data. Please visit *http://www.fasebj.org* to obtain this information.

ticity, regeneration, and repair (20) or participate in pathological events. Retinoic acid (RA), the active metabolite of vitamin A, is an established signaling molecule in vertebrate development. RA plays an important role in cellular patterning, differentiation, and growth signal decoded by retinoic acid receptors (RARα/β/γ), nuclear hormone receptors selective for all-*trans*-RA (atRA). RARs heterodimerize with RXRs (RXRα/β/γ) that bind a spectrum of ligands, including 9-*cis*-RA (9cRA). Liganded RAR/RXR complexes associate with a large number of coactivator proteins to modulate gene expression (21–23). The RA pathway is clearly activated in adult neurogenesis (24), and RA pathway dysfunction is potentially implicated in the pathology of aging, Parkinson's disease, Alzheimer's disease, and schizophrenia (21, 25). Notably, Duncan *et al.* (26) showed that intense light exposure generates atRA and identified an RA-like compound in the neural retina and RPE of P23H-3 transgenic rats. Here, we profile RA signaling in the LIRD retina and find that it converges with α- and β Ca^{2+}/calmodulin-dependent protein kinase II (α- and βCaMKII) signaling, potentially regulating the availability or activity of RXRs. RXR antagonists completely inhibit anomalous neuritogenesis, offering hope for attenuating neural remodeling during retinal degeneration.

MATERIALS AND METHODS

LIRD and subretinal injections

All animals were age matched, with *ad libitum* access to food and water. Except during light-exposure treatment, animals were maintained in dim light (~20 lux) on a 12-h in normal phase (lights on 7 AM to 7 PM). Albino mice (The Jackson Laboratory, Bar Harbor, ME, USA) were mainly used in the LIRD model. Albino mice retinas lack melanin, which protects the retina, probably by the absorption of light, and therefore are particularly sensitive to the deleterious effects of artificial constant light (27). The *Rdh12*$^{-/-}$ mice were generated as described previously (28). The LIRD model was established according to literature (29, 30) with mirror alterations (Supplemental Data and Supplemental Fig. S1). Briefly, adult *Balb/C* albino mice and *Rdh12*$^{-/-}$ mice were exposed to ~2500- to 3000-lux constant visible light for 24 and 96 h, respectively. Subretinal injection was performed based on literature (31, 32) with minor modifications. Briefly, under ketamine-xylazine anesthesia, 0.5 μM RA (atRA+9cRA), 200 μM citral, 5 μM KN-62, 1 μM SR11237, and 10 μM UVI3003 were injected into the subretinal space (central region) of albino mice in 0.5 μl volumes using a 33-gauge microsyringe (Hamilton, Reno, NV, USA) 30 min before light exposure or on post-light-exposure day 7 (pLX7). A successful subretinal injection caused swelling of the retina. Control eyes were injected with vehicle (DMSO).

Primary retinal cell culture

Primary retinal cell cultures were prepared from 9 d postnatal mice and maintained in 2 ml of culture medium (DMEM/F12; Invitrogen, Carlsbad, CA, USA), 0.6% glucose, 0.1125% $NaHCO_3$, 5 mM HEPES, 1% heat-inactivated fetal bovine serum, 1.5 μM thymidine, glutamax (0.5×; Invitrogen), 25 μg/ml insulin (Sigma, St. Louis, MO, USA), 100 μg/ml transferrin (Sigma), 60 μM putrescine (Sigma), 30 nM selenium (Sigma), 20 nM progesterone (Sigma), and penicillin/streptomycin (1×; Invitrogen) (33). Retinas were harvested and dissected in cold HBSS containing 15 mM HEPES, incubated with 0.25% trypsin for 8.5 min at 37°C, and rinsed 3× in 5% DMEM/F12. Retinal cells were seeded (3–6×10^5 cells/ml) into 24-well plates containing poly-L-lysine and laminin-coated glass coverslips, and incubated at 37°C and 5% CO_2. Basic fibroblast growth factor (10 ng/ml) was added 2 h after seeding. When retinal cell confluence was 50–80% after 24 h, RA (atRA+9cRA) was added with the final concentration of 0.05 μM and incubated for 4 d.

HPLC analysis

All tissue preparations and extractions were performed under dim red light. A 2-step acid-base extraction protocol was used to recover RA (34). Retinas from 3 mice were pooled and homogenized 2× in 1 ml of homogenizing beads and 1 ml of 0.05 M KOH/80% methanol plus 0.1% butylated hydroxytoluene using a Mini-Beadbeater homogenizer (BioSpec Products, Bartlesville, OK, USA). Homogenates were extracted twice with 4 ml of hexane:isopropanol (9:1). The remaining aqueous phase was acidified with 80 μl of 4 M HCl and extracted 4× with 4 ml of hexane:isopropanol (9:1); the extracts were combined and dried under nitrogen gas. HPLC mobile phase [70% A (acetonitrile with 0.1% formic acid): 30% B (H_2O with 0.1% formic acid), 70 μl] was added to dissolve the dried film, and 30-μl aliquots were injected onto a Thermo Separations Surveyor HPLC system (Thermo, West Palm Beach, FL, USA) with a UV6000 photodiode array detector and an MSQ single-quadrupole mass spectrometer. HPLC analysis was performed on a C18 column (150×4.6 mm, 2.6 μm; Phenomenex, Torrance, CA, USA) with a linear gradient rising from 70% A:30% B to 95% A:5% B in 20 min at a flow rate of 0.6 ml/min. Identification of atRA was based on retention time, UV absorbance, and mass spectrum. Quantification was based on standard curves of authentic atRA standards injected onto the HPLC system *vs.* integrated UV absorbance of their eluted peaks.

Immunoprecipitation analysis

Retinas were lysed in RIPA buffer (RIPA lysis buffer kit; Santa Cruz Biotechnology, Santa Cruz, CA, USA) for 1 h at 4°C with gentle agitation. Lysates were immunoprecipitated for 1 h at 4°C using specific antibodies (αCaMKII 1:1000, Upstate Biotechnology, Lake Placid, NY, USA; βCaMKII 1:1000, Invitrogen) and protein G agarose beads (Roche, Indianapolis, IN, USA) modified from literature (35). Samples were analyzed by Western blotting.

Western blotting analysis

Protein samples were combined with NuPAGE LDS sample buffer (4×; Invitrogen) and NuPAGE sample reducing agent (10×; Invitrogen), then boiled for 10 min at 95°C. Western blotting analysis was carried out using NuPAGE 4–12% Bis-Tris gels (Invitrogen) at 200 V for 35–40 min. Gels were electroblotted onto PVDF membrane (Millipore, Bedford, MA, USA) for 1.5 h at 25 V using a wet electroblotting system (XCell SureLock Mini-Cell; Invitrogen). Blots were blocked for 1 h in PBS (8 mg/ml NaCl, 0.2 mg/ml KCl 0.2, 1.44 mg/ml Na_2HPO_4, and 0.24 mg/ml KH_2PO_4, pH 7.4) with 0.1% Triton-X100 (pH 7.4; PBST) containing 5% nonfat dry milk (NFDM). Blots were incubated overnight at 4°C in primary antibodies diluted in 5% NFDM-PBST solution

[RARα: 1:1000, Chemicon; RARβ: 1:400, Santa Cruz Biotechnology; RXRα: 1:400, Santa Cruz Biotechnology; RXRβ: 1:1000, Upstate; RXRγ: 1:400, Santa Cruz Biotechnology; cellular retinoic acid binding protein II (CRABPII): 1:200, Santa Cruz Biotechnology; αCaMKII 1:1000; βCaMKII: 1:1000; GluA1: 1:3000, Millipore; GluA2: 1:1000, Millipore]. Blots were washed 3× for 10 min in PBST, incubated for 2 h in secondary antibodies (IgG-HRP, Santa Cruz Biotechnology; 1:5000 in 5% NFDM-PBST) followed by 3 more washes of 10 min in PBST. Immunostaining was revealed by the SuperSignal West Dura Extended Duration Substrate kit (Thermo Scientific, Waltham, MA, USA), and scanned using the Quantity One imaging system (Bio-Rad). Densitometry for each band was measured using ImageJ (U.S. National Institutes of Health, Bethesda, MD, USA). β-Actin was used as a loading control.

Immunohistochemistry and confocal imaging

Whole eyes were removed and rinsed in HBSS, fixed in 4% paraformaldehyde (PFA) for 2 h at 4°C, and then washed with PBS twice for 10 min each. Eyes were incubated in PBS with 20% sucrose for 4 h at 4°C. Serial 12-μm coronal sections were made with a cryostat microtome (Leica CM3050 S; Leica Microsystems, Wetzlar, Germany) and collected on Superfrost/plus microscope slides (Fisher Scientific, Pittsburgh, PA, USA). Cryosections were washed 2× for 10 min in PBS, then blocked with blocking buffer (1× PBS, 0.15% Triton-X100, 2% donkey serum or 2% goat serum, and 0.01% sodium azide) for 30 min. Cultured cells were rinsed 2× for 10 min in PBS, fixed in 4% PFA for 20 min at room temperature, washed 2× for 10 min in PBS, and blocked with blocking buffer for 1 h. Cryosections and fixed cells were incubated overnight at 4°C in primary antibodies diluted in blocking buffer [RARα, 1:200; RARβ, 1:200; RXRα, 1:300; RXRβ, 1:400; RXRγ, 1:200; CRABPII, 1:50; cellular retinaldehyde binding protein (CRALBP), 1:2000 (kindly provided by Dr. John Saari, University of Washington, Seattle, WA, USA); αCaMKII, 1:500; βCaMKII, 1:500; protein kinase C α (PKCα), 1:2000, Sigma; postsynaptic density-95 (PSD-95), 1:1000, Chemicon, Temecula, CA, USA]. After washing 3× for 10 min in PBS, sections and cells were incubated for 45 min at room temperature in secondary antibodies (goat anti-rabbit Cy3, Jackson; goat anti-rabbit 488, Invitrogen; goat anti-mouse Cy3, Chemicon; goat anti-mouse 647, Invitrogen; and donkey anti-goat 488, Invitrogen) diluted 1:1000 in blocking buffer. For double or triple staining, sections and cells were sequentially incubated with primary antibodies and secondary antibodies as above. After incubation with antibodies, sections or cells were washed 3× for 10 min in PBS, then treated with 10 μM DAPI for 5 min at room temperature. Sections and cells were washed 3× for 10 min in PBS and mounted with PermaFluor mounting medium (Thermo). Sections and cells from all groups were processed simultaneously to reduce staining artifacts or intensity differences. Negative controls were performed by omission of the primary antibody. Images of fixed tissue or primary retinal neurons were acquired on an Olympus FV1000 confocal microscope (Olympus, Tokyo, Japan), and neuritogenesis was analyzed as described previously (36–38). In brief, neurite length was measured from the point of emergence at the cell body to the tip of each segment. For studies of *in vivo* neuritogenesis, one section was selected from each animal, and the 20 longest dendrites from 20 rod bipolar cells in a specific region (ventral midperipheral region, 120 μm in length) were measured and calculated as the mean. For studies of *in vitro* neuritogenesis, 3 coverslips/treatment were analyzed in each experiment (~20 cells). Quantification of the morphological parameters was carried out using ImageJ by investigators masked to experimental conditions.

Electron microscopy and overlay microscopy

Conventional transmission electron microscopy was performed as described previously (39) on 90-nm lead-stained sections on single-hole grids. Sections serial to the section reserved for electron microscopy were processed for molecular phenotyping, and the optical RGB images were registered (IR-Tweak; Scientific Computing Institute, University of Utah) to the ultrastructure. Both high- and low-magnification montages were captured as conventional electron micrographs and scanned as 8-bit monochrome channels at 300–600 dpi. Large montages were assembled from the ultrastructural images (NCR toolset; Scientific Computing Institute) and then registered to the scaled optical microscope data (IR-Tweak).

Grating acuity

Grating acuity of animals was measured with a virtual optomotor system as described previously (40). In brief, an optomotor system with a computer program (CerebralMechanics; http://www.cerebralmechanics.com) was used. The mice were tested during their daylight cycle, normally for 5 to 30 min. Mice were placed one at a time on the platform and were habituated for a few minutes before the onset of testing. The gray was set with a low-spatial-frequency (0.1 cyc/deg) sine wave grating (100% contrast) of the same mean luminance and moving in one direction. The process of incrementally changing the spatial frequency of the test grating was repeated until the highest spatial frequency that the mouse could track was identified as the threshold. A contrast-sensitivity function was assessed using the same procedures. The highest spatial frequency tracked in either direction was recorded as threshold. Experimenters were masked to the treatment.

Data analysis

Data are expressed as means ± SE and were analyzed with SPSS 12.0 (SPSS Inc., Chicago, IL, USA) for optometry, neuritogenesis, and levels of atRA. Statistical comparisons were made using Bonferroni tests and analysis of variance (ANOVA); $P < 0.05$ was defined as the level of significance. Protein levels represent pooled data of entire groups and are expressed as means only.

RESULTS

Photoreceptor degeneration triggers anomalous neuritogenesis

Among the downstream victims of rod photoreceptor loss are the rod bipolar cells, readily tracked *via* PKCα immunoreactivity. We used them as surrogate for complex neuritogenesis throughout the retina. LIRD retinas conveniently partition into survivor zones where stressed photoreceptors and retinal neurons survive, yet express explicit remodeling defects, such as neuritogenesis and reprogramming, and light-damage (LD) zones where rods and cones die and retinal neurons undergo extreme remodeling (19). PKCα immunore-

activity mapping showed obvious rod bipolar cell neuritogenesis in the survivor zone, extending their dendrites past the outer plexiform layer (OPL) into the outer nuclear layer (ONL). PSD-95 staining revealed that rod spherules and cone pedicles (41) retracted into the survivor zone ONL (**Fig. 1*A–F***). Subsequently, ectopic microneuromas (the tangles of cell processes), which contain numerous synapses formed *de novo* and possess active synaptic elements corruptive of normal signaling (1), bridged the OPL and inner plexiform layer (IPL) in the survivor zone (Fig. 1*G*). In human retinitis pigmentosa and animal models of human retinitis pigmentosa (15), rod bipolar cells switch their target to cones. Similarly, LIRD induced a shift of PKCα/PSD-95 colocalization to survivor cone pedicles (Fig. 1*C*, *F*). Though photoreceptors and second-order neurons persisted for months in the survivor zone, visual function continued to decline (Fig. 1*H*), which suggests that corruptive neuritogenesis, target switching, and reprogramming progressively impair visual signaling (16, 15).

RA signaling is activated during LIRD

Duncan *et al.* (26) showed that intense light exposure generates atRA in rhodopsin P23H mutant rats. Here, we characterized the RA signaling in detail. The normal retina harbors a large depot of retinoids, bound primarily to photoreceptor opsins at a millimolar scale, or stored as retinylesters in oil droplets in the RPE (42). Photoreceptor degeneration removes the opsin-containing compartment and disrupts the retinoid cycle, but other retinoid binding proteins, such as CRALBP, were still strongly expressed by the RPE and Müller cells and were even up-regulated (**Fig. 2*A***). High-performance liquid chromatography (HPLC) and mass spectrometry analysis showed increased atRA levels early in LIRD (Fig. 2*B–E*). CRABPII is a transcriptional

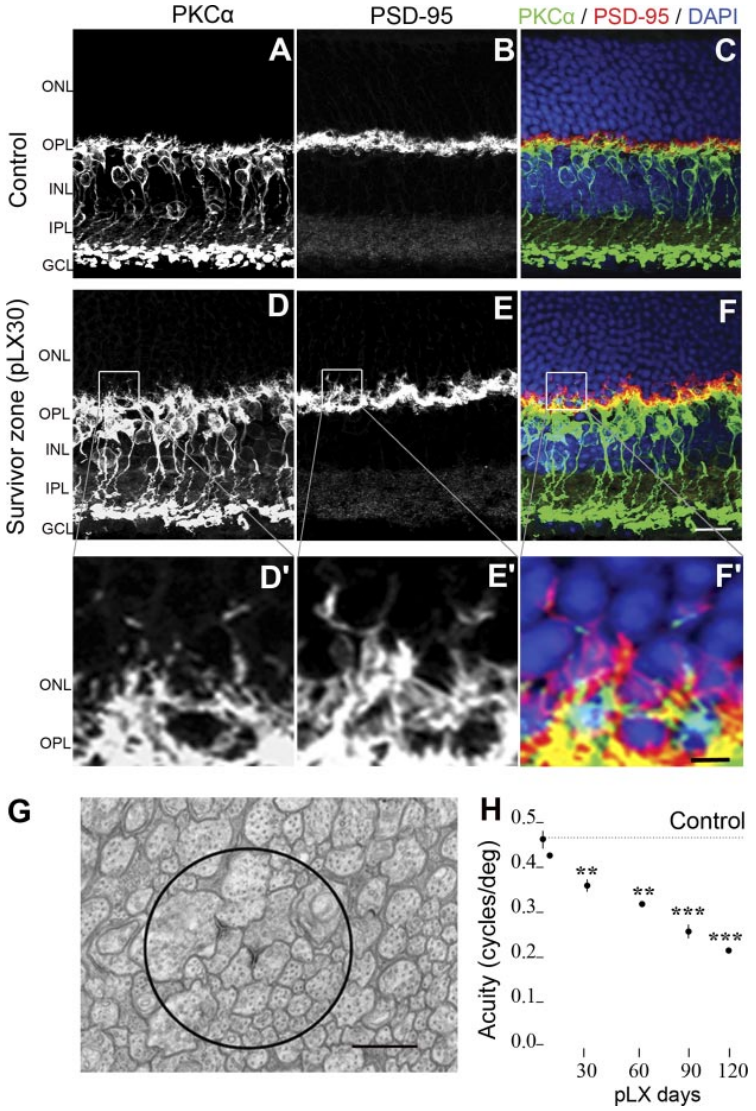

Figure 1. LIRD induces anomalous neuritogenesis. *A–F*) PKCα staining (*A*, *D*) demonstrating early morphological changes in rod bipolar cell dendrites as they extended beyond their normal confines of the OPL into the ONL, while PSD-95 immunoreactivity (*B*, *E*) demonstrated that terminals of photoreceptors were retracted into the ONL in the survivor zone (pLX30). LIRD induced a shift of PKCα/PSD-95 colocalization to survivor cone pedicles (*C*, *F*). *D′–F′*) High-magnification views of boxed areas in *D–F*. *G*) Transmission electron microscopy image of a microneuroma showing a bundle of 100- to 400-nm-thick processes running perpendicularly through this plane of section. Apparent dyad-like synaptic structures bereft of ribbons were present (circle). *H*) Progressive decrease in visual acuity of the LIRD mouse, $n = 5$. $^{**}P < 0.01$, $^{***}P < 0.001$ *vs.* control. Scale bars = 20 μm (*A–F*); 4 μm (*D′–F′*); 1 μm (*G*).

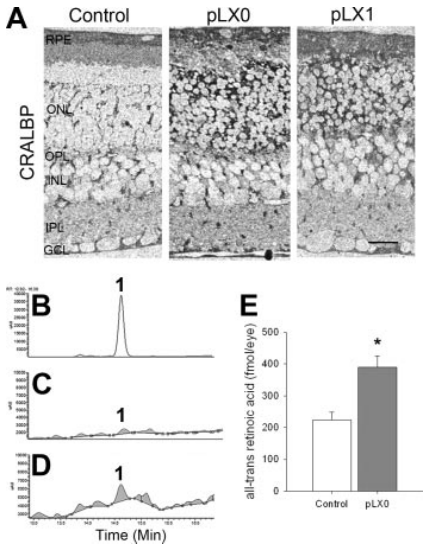

Figure 2. CRALBP and atRA levels are increased during LIRD. *A*) CRALBP immunohistochemistry in the LIRD retinas, demonstrating increased levels at light damage onset. Scale bar = 20 μm. *B–D*) atRA concentrations increase during LIRD. Typical HPLC chromatograms of atRA standard (*B*), control (*C*), and LIRD retinas (pLX0; *D*). Peak 1 denotes atRA. *E*) Quantification analysis showed an increase in atRA levels during LIRD. $*P < 0.05$ *vs.* control, $n = 9$.

coactivator that channels RA to the receptor complex (43–45), thus sensitizing cells to RA and tracking RA signaling. CRABPII promoter harbors RA response elements (46), establishing CRABPII as an RA sensor. Normal mouse retina expressed nuclear CRABPII in the ganglion cell layer (GCL) and inner nuclear layer (INL), and CRABPII levels increased immediately following LIRD exposure, but were almost undetectable by pLX7 (**Fig. 3*A–C***), suggesting transient RA production. Normal mouse retina also expressed nuclear RXRα/β/γ, and RARα/β in the GCL and INL were highly colocalized with RXRα/β/γ (Fig. 3*D–I*), supporting the potential for heterodimerization. RARs and RXRs showed normal distributions in the survivor zone. Many signals were transient as shown by Western blotting. RARβ, RXRα, and RARγ levels increased during LIRD, while RARα and RXRβ levels showed no change (Fig. 3*J, K*). We further demonstrated RAR and RXR immunoreactivity in PKCα immunoreactive cells in primary retinal neuron cultures (**Fig. 4**), proving that rod bipolar cells express RA signaling. All these results suggest a role of RA signaling in the initiation of neuritogenesis by rod bipolar cells.

Exogenous RA leads to neuritogenesis

RA treatment led to exuberant neurite outgrowth in primary cultured rod bipolar cells (**Fig. 5**), spontaneous *in vivo* neuritogenesis by rod bipolar cells in control mice, and accelerated neuritogenesis in LIRD mice, where rod bipolar cell dendrites extended halfway into the ONL (**Fig. 6*A–D, H***). RA injection with vehicle had no obvious effect on neuritogenesis in the ventral midperipheral region (Fig. 6*A*). RA injection at pLX7, when CRABPII had nearly disappeared, had no effect on neuritogenesis (Fig. 6*E, H*), which suggests a critical

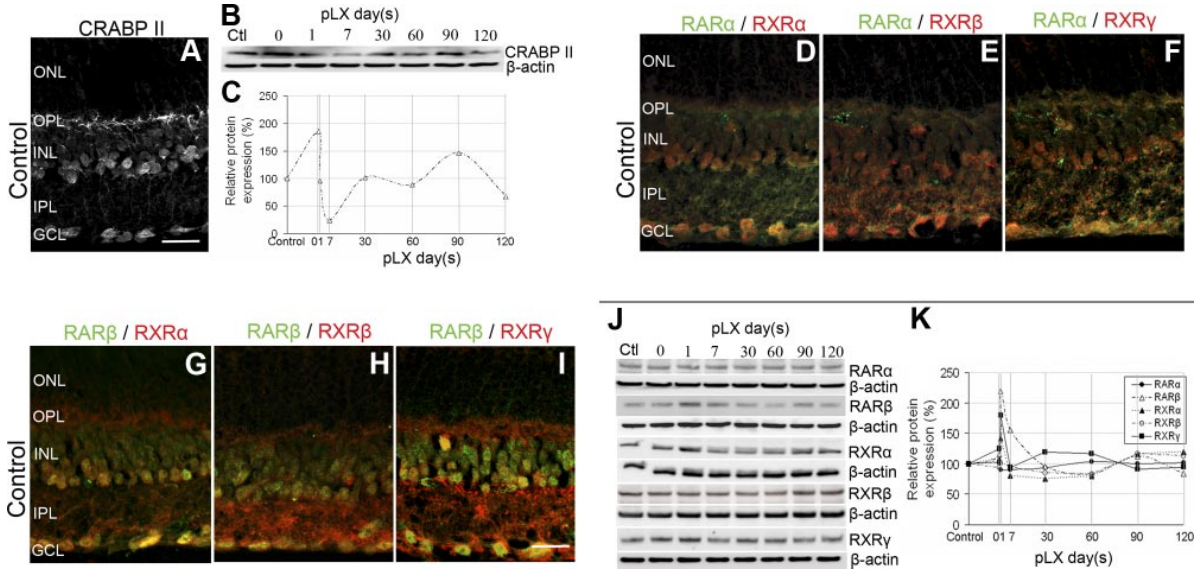

Figure 3. RA signaling is present in adult retinas and activated during LIRD. *A*) CRABPII was observed in the INL and GCL of control retinas. *B, C*) Western blots (*C*) and data quantification (*D*) showed that CRABPII levels increased immediately following LIRD, but reduced to almost undetectable levels by pLX7 before oscillating around normal levels from pLX30 to pLX120, $n = 9$. *D–I*) RARα (*D–F*), RARβ (*G–I*), RXRα (*D, G*), RXRβ (*E, H*), RXRγ (*F, I*), and colocalization of RARs/RXRs were observed in the INL and GCL of control retinas. *J–K*) Western blots (*J*) and data quantification (*K*) showed that RA signaling was activated during LIRD. RARβ, RXRα, and RARγ levels increased, while RARα and RXRβ levels showed no change, $n = 9$. Scale bars = 20 μm.

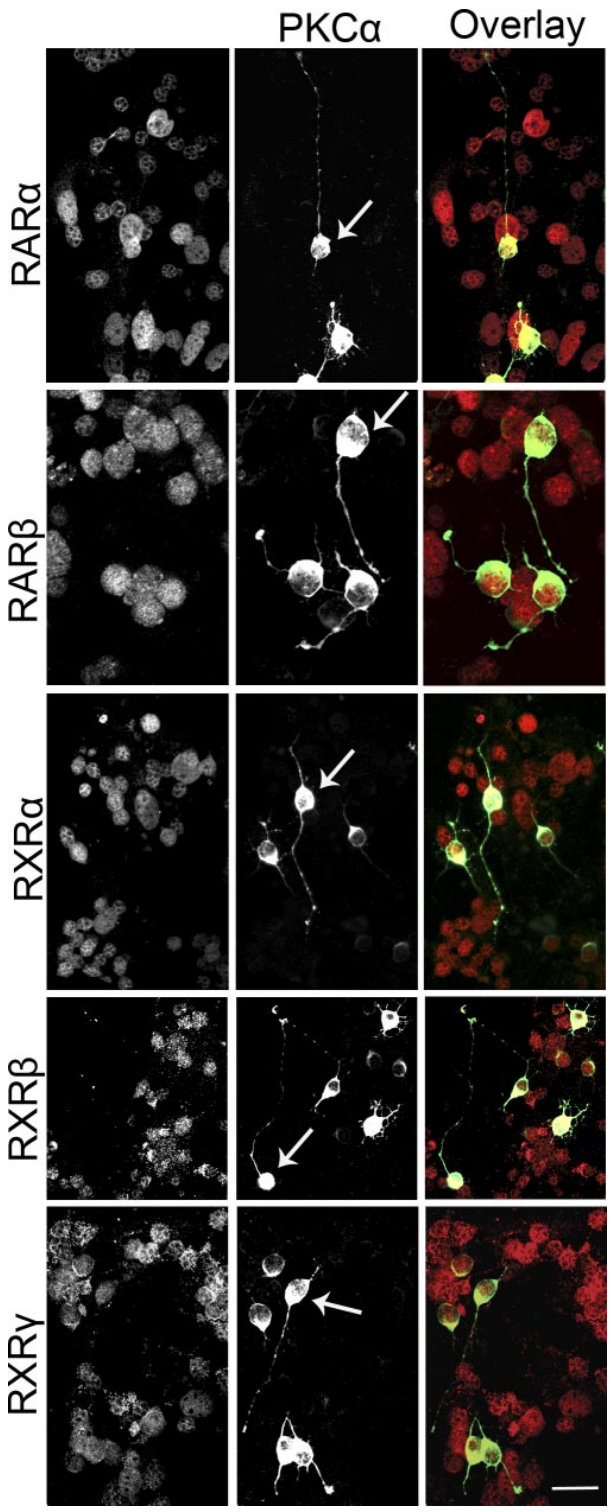

Figure 4. RARα/β and RXRα/β/γ are expressed in rod bipolar cells. RARα/β and RXRα/β/γ were expressed in the nuclei, while PKCα was expressed in the cell body and neurites. Among the RARα/β$^+$ and RXRα/β/γ$^+$ retinal neurons, some cells were PKCα$^+$. Some amacrine cells were also PKCα$^+$ but were easily differentiated from rod bipolar cells (arrows) by morphology. Scale bar = 20 μm.

channeling role of CRABPII in RA signaling, as seen in adipocytes (47). Citral is a potent inhibitor of aldehyde dehydrogenases (ALDHs) responsible for the *in vivo* production of RA (48). Our study showed that citral only partially attenuated neuritogenesis in LIRD mice (Fig. 6*F*, *H*) if administered 30 min prior to light stress, which suggests that other signaling pathways may participate in neuritogenesis during retinal degeneration. When citral was administered at pLX7, it had no effect on neuritogenesis (Fig. 6*G*, *H*), which underscores the transient nature of RA signaling in LIRD. Similarly, LIRD *Rdh12*$^{-/-}$ mice, in which retinoid levels are significantly decreased (49), showed decreased levels of neuritogenesis compared with heterozygous LIRD *Rdh12*$^{+/-}$ mice (Fig. 6*I*–*L*). These findings suggest that RA is sufficient to induce neuritogenesis.

LIRD activates CaMKII signaling

Our next question was what the partners of RA signaling might be or which signaling is involved in neuritogenesis during retinal degeneration. We then studied the role of CaMKII in neuritogenesis. CaMKII plays a central role in synaptic plasticity; both α- and βCaMKII are neuron-specific and expressed in retinal neurons (50). LIRD selectively evoked a rapid increase in βCaMKII levels but had no obvious effect on αCaMKII levels (**Fig. 7*A*, *B***). LIRD mice also showed increases in low calcium permeability GluA2 AMPA receptor subunit expression but no change in high calcium permeability GluA1 subunits (Fig. 7*C*, *D*). Combined with deafferentation due to photoreceptor loss and concomitant decreases in mGluR6 signaling (18), light signaling in retinal degeneration should be blunted. Notably, the CaMKII inhibitor KN-62 (mimicking a low-Ca^{2+} environment) accelerated neuritogenesis (Fig. 7*E*–*G*), suggesting the involvement of CaMKII in neuritogenesis during retinal degeneration. Consistently, LIRD *Rdh12*$^{-/-}$ mice that showed lower neuritogenesis had lower protein levels of βCaMKII compared with *Rdh12*$^{+/-}$ mice. However, LIRD *Rdh12*$^{-/-}$ and *Rdh12*$^{+/-}$ mice demonstrated no difference in αCaMKII levels (Fig. 7*H*, *I*).

α- and βCaMKII interact with and regulate RXRs

What is the link between activity and RA signaling? CaMKIIγ regulates RARα transcription in myeloid leukemia cells (51), so we tested for interactions in retina. Antibodies against CaMKII immunoprecipitated RXRα/β/γ but not RARα/β (**Fig. 8*A***), suggesting that CaMKII may regulate the availability of RXRs for coactivation events. Notably, modulation of RXRs directly influenced neuritogenesis. The RXR agonist SR11237 was more potent than RA in activating neuritogenesis in control and LIRD mice, and no significant difference was found between the SR11237 group and the pLX21 + SR11237 group (Fig. 8*B*, *C*, *E*). However, RXR antagonist UVI3003, which renders the RXR subunit transcriptionally inactive (52), completely prevented neuritogenesis (Fig. 8*D*, *E*),

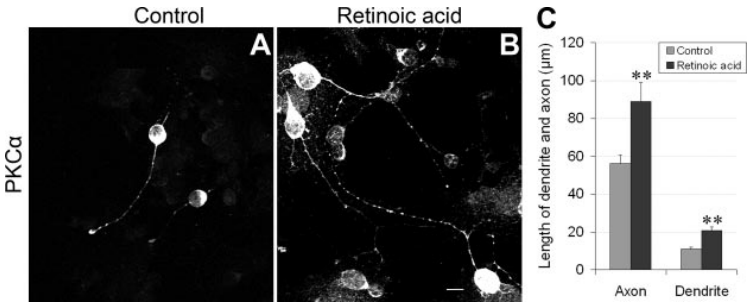

Figure 5. Exogenous RA administration promotes rod bipolar cell neurite outgrowth. *A*, *B*) Retinal neurons from control (*A*) and RA (atRA+9cRA)-treated primary cell cultures (*B*) were immunostained for PKCα. Scale bar = 10 μm. *C*) Quantitative comparisons showed that RA significantly increased the length of both dendrites and axons of rod bipolar cells. $^{**}P < 0.01$ *vs.* control.

which suggests that RXRs are in the final common path. Thus, we uncovered the mechanisms leading to neuritogenesis during retinal degeneration (**Fig. 9**).

DISCUSSION

The first consequence of light absorption by rhodopsin in the retina is the generation of all-*trans*-retinaldehyde and its rapid conversion to all-*trans*-retinol. RA is generated from all-*trans*-retinol biogenically, as a consequence of retinol dehydrogenase (RDH) and ALDH enzymatic activities in the retina (53). Given that RA signaling elements are abundant in the neural retina, it is not surprising that RA is detectable in the neural retina after inherited degenerations (26, 54) and in LIRD mice. We found activation in RA signaling in LIRD mice. Previous studies reported that even 10 min of intense light exposure causes a doubling in retinal atRA (34). Elevation of RA has also been reported in *Mitf*^{vit} (vitiligo) mice of retinal degeneration (54). These findings suggest that activation in RA signaling may be a common mechanism in retinal degeneration, regardless of the initiating event (light) or gene defect. As CRABPII expression is up-regulated by RA (46), the early spike in CRABPII expression is further evidence for increased endogenous RA availability. Exogenous RA initiates neurite outgrowth in control and primary retinal cell cultures. Then it is reasonable that increases in RA levels during retinal degeneration will trigger anomalous neuritogenesis and network formation. The role of RA in neurite remodeling is further proved by its effect on the formation of spinules by horizontal cells in carp kept in complete darkness (55). RA also induces neurite outgrowth in invertebrate neurons (*Lymnaea stagnalis* central ring ganglia culture), which suggests that these actions of RA on neuritogenesis are

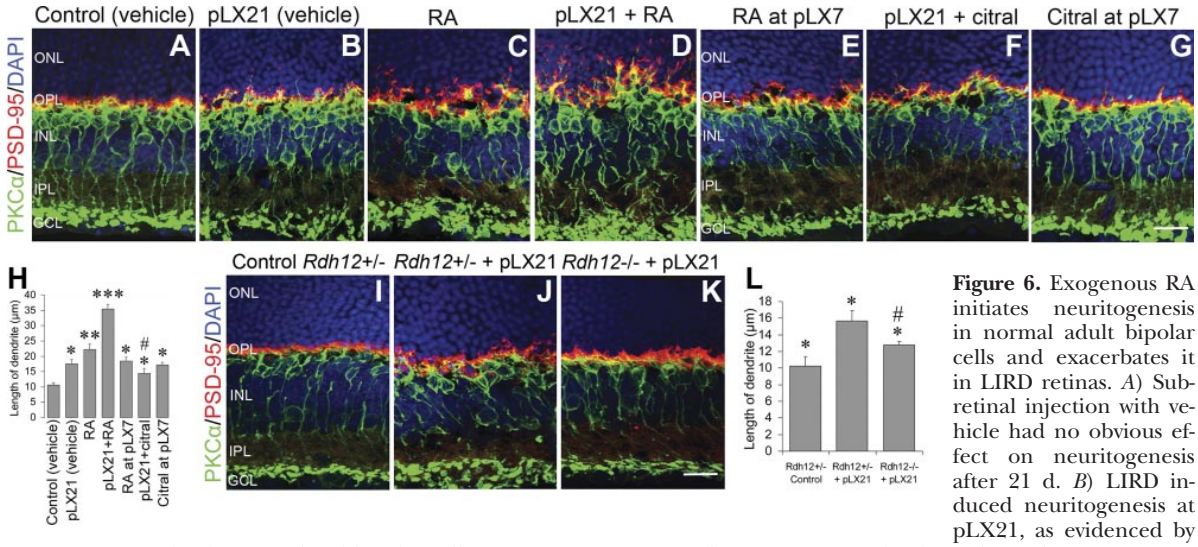

Figure 6. Exogenous RA initiates neuritogenesis in normal adult bipolar cells and exacerbates it in LIRD retinas. *A*) Subretinal injection with vehicle had no obvious effect on neuritogenesis after 21 d. *B*) LIRD induced neuritogenesis at pLX21, as evidenced by PKCα staining. *C*) RA initiated rod bipolar cell neuritogenesis in control mouse retinas. *D*) RA accelerated neuritogenesis in LIRD mouse retinas. *E*) RA had no effect on neuritogenesis when it was injected at pLX7. *F*) Partial inhibition of neuritogenesis by citral in LIRD mouse retinas. *G*) Citral had no effect on neuritogenesis when it was injected at pLX7. *B–G*) Terminals of photoreceptors (PSD-95 staining) were retracted to the ONL paralleling with neuritogenesis by rod bipolar cells. *H*) Summary data (means±SE) for the length of rod bipolar cell dendrites, $n = 5$. $^{*}P < 0.05$, $^{**}P < 0.01$, $^{***}P < 0.001$ *vs.* control (vehicle); $^{\#}P < 0.05$ *vs.* pLX21 (vehicle). *I–K*) Rates of neuritogenesis were slower in LIRD *Rdh12*$^{-/-}$ mice compared with LIRD *Rdh12*$^{+/-}$ mice. PKCα and PSD-95 staining was normal in control *Rdh12*$^{+/-}$ retinas (*I*) but demonstrated LIRD-induced neuritogenesis in the survivor zones of both *Rdh12*$^{+/-}$ (*J*) and *Rdh12*$^{-/-}$ retinas (*K*). *L*) Compared to LIRD *Rdh12*$^{+/-}$ mice, neuritogenesis in LIRD *Rdh12*$^{-/-}$ mice was less obvious. $^{*}P < 0.05$ *vs.* control *Rdh12*$^{+/-}$; $^{\#}P < 0.05$ *vs.* *Rdh12*$^{+/-}$ + pLX21. Scale bars = 20 μm.

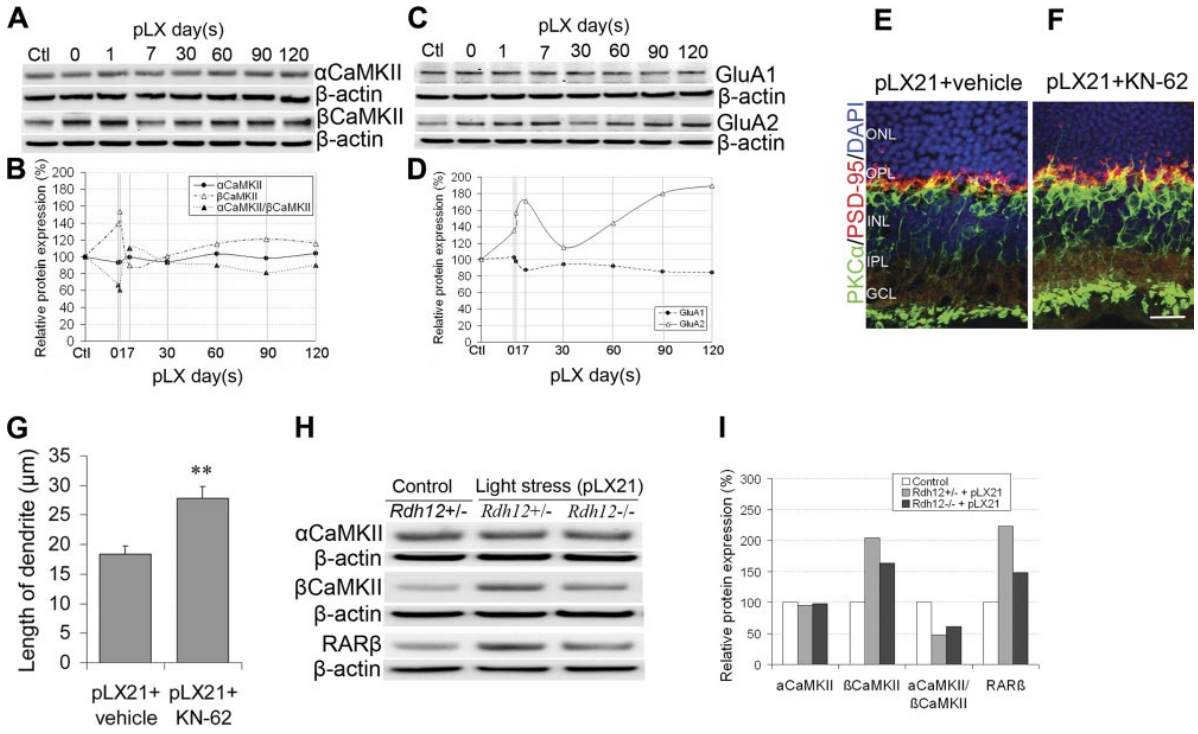

Figure 7. CaMKII signaling is involved in neuritogenesis during LIRD. *A*, *B*) Western blots (*A*) and data quantification (*B*) showed that LIRD increased βCaMKII protein levels, while αCaMKII protein levels showed no change. Ratio of αCaMKII/βCaMKII proteins decreased, $n = 9$. *C*, *D*) Western blots (*C*) and data quantification (*D*) showed that LIRD increased the protein levels of GluA2, but GluA1 levels showed no change, $n = 9$. *E*, *F*) KN-62 (*F*) accelerated neuritogenesis compared to vehicle (*E*). Scale bar = 20 μm. *G*) Summary data (means±SE) for the length of rod bipolar cell dendrites. $^{**}P < 0.01$ *vs.* pLX21 (vehicle), $n = 5$. *H*, *I*) Western blots (*H*) and data quantification (*I*) showed that LIRD had no effect on the protein levels of αCaMKII but increased the protein levels of βCaMKII and RARβ, especially in *Rdh12*$^{+/-}$ mice. Ratio of αCaMKII to βCaMKII proteins was therefore reduced; $n = 3$.

highly conserved across species (56). Because neuritogenesis by rod bipolar cells was noted in animals older than 1 yr (37), the effect of aging on neuritogenesis in our study should be excluded (~3 mo).

In normal retina, neuronal ALDH likely encounters little retinaldehyde, but photoreceptor loss provides an opportunity for abundant access to RPE- or Müller cell-derived retinaldehyde. In this scenario, the triggering of neuritogenesis by RA would be pathological rather than homeostatic. The spike in RA corresponds with transient CRABPII expression, suggesting that direct anti-RA therapies may have impractically narrow therapeutic windows in coherent models. However, many forms of retinitis pigmentosa involve prolonged, geometrically complex photoreceptor loss, so that RA triggering may be ongoing. Direct measures of RA

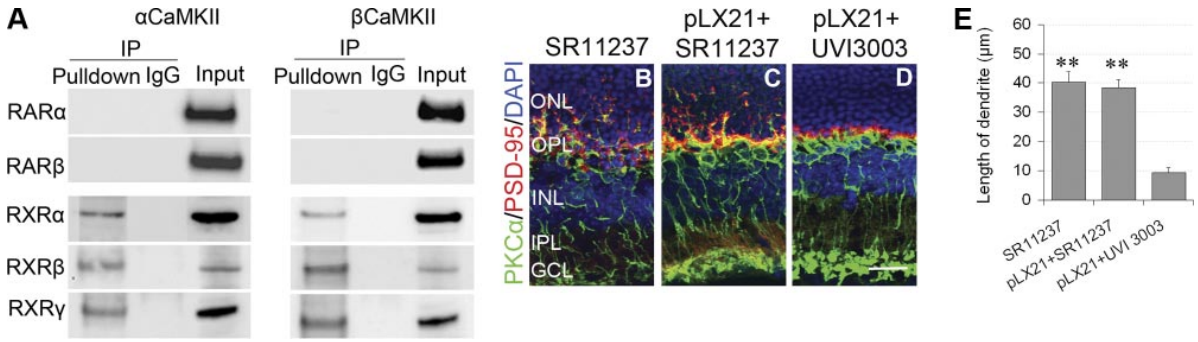

Figure 8. α- and βCaMKII regulate the activity of RXRs during retinal degeneration. *A*) α/βCaMKII directly interacted with RXRα/β/γ, but not RARα/β, in mouse retinas. *B, C*) SR11237 initiated rod bipolar cell neuritogenesis in control mouse retinas (*B*), and accelerated neuritogenesis in LIRD mice retinas (*C*). *D*) UVI3003 completely inhibited neuritogenesis. Scale bar = 20 μm. *E*) Summary data (means±SE) for the length of rod bipolar cell dendrites, $n = 5$. $^{**}P < 0.01$ *vs.* UVI3003 group.

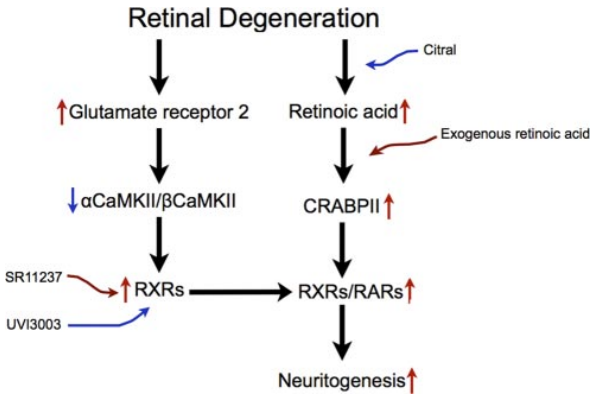

Figure 9. Schematic mechanisms leading to neuritogenesis during retinal degeneration. Activation in RA signaling, including RA, CRABPII, and RARs/RXRs, activates neuritogenesis during LIRD. Exogenous administration of RA initiates neuritogenesis in control mouse retinas and accelerates neuritogenesis in LIRD mouse retinas, while citral partially inhibits its neuritogenesis. Meanwhile, RXRs directly interact with αCaMKII and βCaMKII, and the activity of RXRs is regulated by CaMKII signaling. LIRD up-regulates the AMPAR GluA2 subunit and decreases the ratio of αCaMKII/βCaMKII proteins, which increases the activity of RXRs. RXR agonist SR11237 initiates neuritogenesis, while RXR antagonist UVI3003 completely prevents neuritogenesis.

signaling in human retinitis pigmentosa tissue would be immensely valuable. In contrast to the transient occurrence of RA signaling, neuritogenesis is enduring. Citral injection 30 min prior to light stress is effective, but when injected at pLX7, it can no longer attenuate neuritogenesis, which persists to at least pLX120 in our experiment. This suggests that largely irreversible downstream pathways are activated.

LIRD clearly attenuates glutamate signaling (due to photoreceptor loss) by increasing the expression of GluA2. This protective response decreases the Ca^{2+} permeability of the entire AMPA receptor complex and prevents GluA1 subunit phosphorylation-dependent increases in AMPA receptor conductance (57, 58). Increasing the ratio of GluA2 subunits in iGluRs could potentially play a role in neuritogenesis by decreasing Ca^{2+} loads in neurons. In contrast, sustained elevation of intracellular Ca^{2+} in response to GluR activation results in depolymerization of microfilaments and microtubules, leading to dendrite outgrowth cessation and regression (59). CaMKII senses cytosolic Ca^{2+} fluxes, which are largely mediated by glutamate-activated AMPA or NMDA receptors in CNS neurons (60), but also likely by mGluR6 receptors in rod bipolar cells (18). αCaMKII is activated by high Ca^{2+} levels, while βCaMKII is more sensitive to lower levels, and heteromeric CaMKII Ca^{2+} responsivity and activity depends on the α/β subunit ratio (61). Decreases in neuronal activity decrease the CaMKII α/β ratio, likely by up-regulating transcription of βCaMKII (62), which positively correlates with the increase in low calcium permeability GluA2 expression in our study. α- and β-CaMKII isoforms have markedly different roles in neuronal plasticity, with αCaMKII regulating synaptic strength and βCaMKII controlling the dendritic morphology and number of synapses (63). Therefore, our results indicate decreased retinal activity during early LIRD, and highlight the important role of glutamate signaling and CaMKII in regulating neuritogenesis.

Blocking neuronal activity by tetrodotoxin (TTX) increases neuronal RA levels (36). Here we also show increased levels of RA during early LIRD. Further, we demonstrate that RA and CaMKII pathways converge at RXRs in LIRD neuritogenesis. α- and βCaMKII interacted with RXRs, not RARs. It may be that RXRs themselves function predominantly, if not exclusively, as critical auxiliary receptors that enhance signaling of many nuclear receptors, including RARs (64). In contrast, RARs seem to operate effectively only as heterodimeric RAR/RXR complexes (65). The interaction suggests that CaMKII signaling may regulate the activity of RXRs, although the motif where RXRs and CaMKII interacts remains unknown. Enhanced βCaMKII expression would ultimately enhance RXR activity and neuritogenesis. This is confirmed by our findings that CaMKII inhibitor KN-62 enhances neuritogenesis, while RXRs antagonists completely inhibit neuritogenesis. Similarly, CaMKII inhibitor KN-62 enhances RAR transcriptional activity in myeloid leukemia cells (51) and prevents retraction of spinules of horizontal cells in *vivo* (66). The similar effects of RA and KN-62 on the formation of spinules by horizontal cells (55, 66) further confirm crosstalk between RA and CaMKII signaling pathways. Given the more extensive partnering of RXRs with other ligands and nuclear receptors, the persistence of neuritogenesis may have other yet undiscovered drivers. Nevertheless, our results suggest that RXRs are in the final common path.

The full consequences of retinal degeneration for retinoid metabolism are unclear. But it is certain that prolonged bleaching events can release very high levels of all-*trans*-retinal, which is potentially retinotoxic (67). Rod photoreceptor outer segments are estimated to contain 3–5 mM rod opsin (68) based on protein mass, but the effective membrane concentration is likely much higher (69), representing a massive depot for 11-*cis*-retinal provisioned by the RPE. Under normal homeostasis, most all-*trans*-retinal formed by bleaching is converted to 11-*cis*-retinol by photoreceptor RDH, and little or none appears to reach the neural retina, consistent with the absence of detectable neuritogenesis in the normal retina. However, coincident with the rapid degeneration of photoreceptors in either light damage or retinal degeneration, it is evident that sufficient all-*trans*-retinal reaches cells containing ADH to result in RA production, consistent with prior reports (26) and our finding of elevated RA-like species in retinal degeneration. Given that the RA dissociation constant for the coactivator CRABP-II is on the order of 2 nm (70), even access to as little as 10^{-6} of the normal all-*trans*-retinal pool should be enough to strongly activate neural RA response elements. Considering the insensitivity of molecular assay methods, the detection

in RA in LIRD retinas implies that a high RA level (based on the affinities of nuclear receptors) is evoked by retinal degenerations. The activation of RAR/RXR signaling is clearly a major component of the remodeling that accompanies retinal degenerations. What can be done about it? Indeed, why even bother?

We used the accessible, sensitive, and rapid phenotype of rod bipolar cell dendrite remodeling to assess neuritogenesis in the LIRD model. However, true retinitis pigmentosa manifests a slower, more pervasive, and complex neuritogenesis that includes anomalous fasiculation and microneuroma formation by bipolar, amacrine, and ganglion cells. These pose severe challenges to interventions (71). Two late-stage downstream approaches could potentially bypass some remodeling defects: epiretinal prostheses (72) and optogenetic targeting of retinal ganglion cells (73, 74). However, it is unlikely that ganglion cell excitation *via* prosthetics or channelrhodopsins can ever be isolated from local networks that drive ganglion cells. Direct synaptic activation of bipolar and amacrine cells by field currents is likely (75), and heterocellular amacrine cell-ganglion cell coupling is abundant in mammalians (76). If microneuromas are the primary sources of photopsias (4) and trigger anomalous excitation waves in rodent models of RP (77), then attenuation of neuritogenesis may significantly improve downstream intervention outcomes. Conversely, upstream interventions, such as suprachoroidal or subretinal implants (78, 79), fetal transplants into the subretinal space (80), and optogenetic interventions targeting remnant cones (81) or bipolar cells (82), all depend on the integrity of downstream connectivity to generate visual signals. Indeed, the poor visual outcomes of even the most surgically successful subretinal implants cannot be readily explained. It is clear that late-stage retinas can be extremely corrupted by neuritogenesis and that many patients may not be candidates for intervention. In those instances, attenuation of neuritogenesis may be essential, and RAR/RXR antagonists are a logical place to start, considering the significant development of RAR/RXR modulators in cancer therapeutics (83, 84).

Strategies to attenuate neuritogenesis with RXR antagonists, such as UVI 3003, are now being assessed in animal models of human adRP. Those studies should determine windows of opportunity for intervention. LIRD rodents display a very coherent photoreceptor stress event spanning only a few days and an apparent RAR/RXR signaling epoch of similar duration. In contrast, human RP remodeling is likely continuous and heterogeneous over retinal space (15). Thus, neuritogenesis in RP is likely ongoing, rather than a precisely timed event. Any attentuation of neuritogenesis, especially when macular vision is at risk, is potentially beneficial or even essential. In practice, these interventions are likely to take the form of periodic intravitreal injections similar to treatments for neovascular AMD.

The LIRD model, because of its unique mimicry of remodeling in retinal disease and its extremely stereotyped and coherent kinetics, has facilitated discovery of key mechanisms underlying pathological neuritogenesis common to retinal degenerations. It may be a powerful surrogate system for the study of CNS rewiring neuropathologies in general. Our observations show that RXRs play a critical role in the pathological process of retinal remodeling and suggest that anti-RXR therapies have the potential to attenuate neuritogenesis and, perhaps, network remodeling *via* microneuromas. This capability would strongly enhance or enable diverse human therapeutic interventions in retinitis pigmentosa and AMD that have been, to date, marginally effective. FJ

This project was supported by U.S. National Eye Institute grants EY002576, EY015128, and EY014800 Vision Core (R.E.M.), EY08123 and EY019298 (W.B.); Research to Prevent Blindness (R.E.M. and B.W.J.); the Edward N. and Della L. Thome Memorial Foundation (B.W.J.), a Moran Eye Center Tiger Team Translational Medicine Award (B.W.J.), Fight For Sight (Y.H.L.), the Knights Templar Eye Foundation (Y.H.L.), the International Retinal Research Foundation (Y.H.L.), and a center grant by the Foundation Fighting Blindness, Inc. (Columbia, MD, USA), to the University of Utah. The authors thank Changjiang Zou for assisting with cell culture and immunoprecipitation; Dr. Ning Tian and Dr. Yingbin Fu for advice on manuscript revision; Cecilia Gerstner for breeding the *Rdh12* mutation mice; Dr. Bala Ambati for assistance with retinal injection; Dr. Felix Vazquez-Chona for advice on manuscript organization; and Drew Ferrell for assistance on imaging.

REFERENCES

1. Jones, B. W., Watt, C. B., Frederick, J. M., Baehr, W., Chen, C. K., Levine, E. M., Milam, A. H., Lavail, M. M., and Marc, R. E. (2003) Retinal remodeling triggered by photoreceptor degenerations. *J. Comp. Neurol.* **464,** 1–16
2. Fariss, R. N., Li, Z. Y., and Milam, A. H. (2000) Abnormalities in rod photoreceptors, amacrine cells, and horizontal cells in human retinas with retinitis pigmentosa. *Am. J. Ophthalmol.* **129,** 215–223
3. Sullivan, R. K., Woldemussie, E., and Pow, D. V. (2007) Dendritic and synaptic plasticity of neurons in the human age-related macular degeneration retina. *Invest. Ophthalmol. Vis. Sci.* **48,** 2782–2791
4. Marc, R. E., Jones, B. W., Watt, C. B., and Strettoi, E. (2003) Neural remodeling in retinal degeneration. *Prog. Retin. Eye Res.* **22,** 607–655
5. Marc, R. E., and Jones, B. W. (2003) Retinal remodeling in inherited photoreceptor degenerations. *Mol. Neurobiol.* **28,** 139–147
6. Elliott, R. C., Miles, M. F., and Lowenstein, D. H. (2003) Overlapping microarray profiles of dentate gyrus gene expression during development- and epilepsy-associated neurogenesis and axon outgrowth. *J. Neurosci.* **23,** 2218–2227
7. Morimoto, K., Fahnestock, M., and Racine, R. J. (2004) Kindling and status epilepticus models of epilepsy: rewiring the brain. *Prog. Neurobiol.* **73,** 1–60
8. Dadon-Nachum, M., Melamed, E., and Offen, D. (2010) The "dying-back" phenomenon of motor neurons in ALS. *J. Mol. Neurosci.* **43,** 470–477
9. Scheibel, A. B., and Tomiyasu, U. (1978) Dendritic sprouting in Alzheimer's presenile dementia. *Exp. Neurol.* **60,** 1–8
10. Li, S., Overman, J. J., Katsman, D., Kozlov, S. V., Donnelly, C. J., Twiss, J. L., Giger, R. J., Coppola, G., Geschwind, D. H., and Carmichael, S. T. (2010) An age-related sprouting transcriptome provides molecular control of axonal sprouting after stroke. *Nat. Neurosci.* **13,** 1496–1504

11. Larner, A. J. (1995) Axonal sprouting and synaptogenesis in temporal lobe epilepsy: possible pathogenetic and therapeutic roles of neurite growth inhibitory factors. *Seizure* **4,** 249–258
12. Deller, T., Haas, C. A., Freiman, T. M., Phinney, A., Jucker, M., and Frotscher, M. (2006) Lesion-induced axonal sprouting in the central nervous system. *Adv. Exp. Med. Biol.* **557,** 101–121
13. Jones, B. W., Marc, R. E., Watt, C. B., Vaughan, D. K., and Organisciak, D. T. (2006) Neural plasticity revealed by light-induced photoreceptor lesions. In *Retinal Degenerative Diseases* (Hollyfield, J. G., Anderson, R. E., and LaVail, M. M., eds) pp. 405–410, Springer, New York
14. Marc, R. E., Jones, B. W., and Watt, C. B. (2006) Retinal remodeling: circuitry revisions triggered by photoreceptor degeneration. In *Plasticity in the Visual System: From Genes to Circuits* (Pinaud, R., Tremere, L. A., and de Weerd, P., eds) pp. 33–54, Springer, New York
15. Marc, R. E., Jones, B. W., Anderson, J. R., Kinard, K., Marshak, D. W., Wilson, J. H., Wensel, T., and Lucas, R. J. (2007) Neural reprogramming in retinal degeneration. *Invest. Ophthalmol. Vis. Sci.* **48,** 3364–3371
16. Jones, B. W., and Marc, R. E. (2005) Retinal remodeling during retinal degeneration. *Exp. Eye Res.* **81,** 123–137
17. Strettoi, E., Porciatti, V., Falsini, B., Pignatelli, V., and Rossi, C. (2002) Morphological and functional abnormalities in the inner retina of the rd/rd mouse. *J. Neurosci.* **22,** 5492–5504
18. Puthussery, T., Gayet-Primo, J., Pandey, S., Duvoisin, R. M., and Taylor, W. R. (2009) Differential loss and preservation of glutamate receptor function in bipolar cells in the rd10 mouse model of retinitis pigmentosa. *Eur. J. Neurosci.* **29,** 1533–1542
19. Marc, R. E., Jones, B. W., Watt, C. B., Vazquez-Chona, F., Vaughan, D. K., and Organisciak, D. T. (2008) Extreme retinal remodeling triggered by light damage: implications for age related macular degeneration. *Mol. Vis.* **14,** 782–806
20. Gage, F. H. (2000) Mammalian neural stem cells. *Science* **287,** 1433–1438
21. Maden, M. (2007) Retinoic acid in the development, regeneration and maintenance of the nervous system. *Nat. Rev. Neurosci.* **8,** 755–765
22. Hyatt, G. A., and Dowling, J. E. (1997) Retinoic acid. A key molecule for eye and photoreceptor development. *Invest. Ophthalmol. Vis. Sci.* **38,** 1471–1475
23. Clagett-Dame, M., McNeill, E. M., and Muley, P. D. (2006) Role of all-trans retinoic acid in neurite outgrowth and axonal elongation. *J. Neurobiol.* **66,** 739–756
24. Jacobs, S., Lie, D. C., DeCicco, K. L., Shi, Y., DeLuca, L. M., Gage, F. H., and Evans, R. M. (2006) Retinoic acid is required early during adult neurogenesis in the dentate gyrus. *Proc. Natl. Acad. Sci. U. S. A.* **103,** 3902–3907
25. Maden, M. (2002) Retinoid signalling in the development of the central nervous system. *Nat. Rev. Neurosci.* **3,** 843–853
26. Duncan, T., Wiggert, B., Whittaker, N., Darrow, R., and Organisciak, D. T. (2006) Effect of visible light on normal and P23H-3 transgenic rat retinas: characterization of a novel retinoic acid derivative present in the P23H-3 retina. *Photochem. Photobiol.* **82,** 741–745
27. Wasowicz, M., Morice, C., Ferrari, P., Callebert, J., and Versaux-Botteri, C. (2002) Long-term effects of light damage on the retina of albino and pigmented rats. *Invest. Ophthalmol. Vis. Sci.* **43,** 813–820
28. Maeda, A., Maeda, T., Imanishi, Y., Sun, W., Jastrzebska, B., Hatala, D. A., Winkens, H. J., Hofmann, K. P., Janssen, J. J., Baehr, W., Driessen, C. A., and Palczewski, K. (2006) Retinol dehydrogenase (RDH12) protects photoreceptors from light-induced degeneration in mice. *J. Biol. Chem.* **281,** 37697–37704
29. Organisciak, D. T., and Vaughan, D. K. (2010) Retinal light damage: mechanisms and protection. *Prog. Retin. Eye Res.* **29,** 113–134
30. Youssef, P. N., Sheibani, N., and Albert, D. M. (2011) Retinal light toxicity. *Eye. (Lond.)* **25,** 1–14
31. Nour, M., Quiambao, A. B., Peterson, W. M., Al-Ubaidi, M. R., and Naash, M. I. (2003) P2Y(2) receptor agonist INS37217 enhances functional recovery after detachment caused by subretinal injection in normal and rds mice. *Invest. Ophthalmol. Vis. Sci.* **44,** 4505–4514
32. Uehara, H., Luo, L., Simonis, J., Singh, N., Taylor, E. W., and Ambati, B. K. (2010) Anti-SPARC oligopeptide inhibits laser-induced CNV in mice. *Vis. Res.* **50,** 674–679
33. Sigulinsky, C. L., Green, E. S., Clark, A. M., and Levine, E. M. (2008) Vsx2/Chx10 ensures the correct timing and magnitude of Hedgehog signaling in the mouse retina. *Dev. Biol.* **317,** 560–575
34. McCaffery, P., Mey, J., and Drager, U. C. (1996) Light-mediated retinoic acid production. *Proc. Natl. Acad. Sci. U. S. A.* **93,** 12570–12574
35. Zhang, H., Constantine, R., Vorobiev, S., Chen, Y., Seetharaman, J., Huang, Y. J., Xiao, R., Montelione, G. T., Gerstner, C. D., Davis, M. W., Inana, G., Whitby, F. G., Jorgensen, E. M., Hill, C. P., Tong, L., and Baehr, W. (2011) UNC119 is required for G protein trafficking in sensory neurons. *Nat. Neurosci.* **14,** 874–880
36. Aoto, J., Nam, C. I., Poon, M. M., Ting, P., and Chen, L. (2008) Synaptic signaling by all-trans retinoic acid in homeostatic synaptic plasticity. *Neuron* **60,** 308–320
37. Liets, L. C., Eliasieh, K., van der List, D. A., and Chalupa, L. M. (2006) Dendrites of rod bipolar cells sprout in normal aging retina. *Proc. Natl. Acad. Sci. U. S. A.* **103,** 12156–12160
38. Guizzetti, M., Moore, N. H., Giordano, G., and Costa, L. G. (2008) Modulation of neuritogenesis by astrocyte muscarinic receptors. *J. Biol. Chem.* **283,** 31884–31897
39. Marc, R. E., and Liu, W. (2000) Fundamental GABAergic amacrine cell circuitries in the retina: nested feedback, concatenated inhibition, and axosomatic synapses. *J. Comp. Neurol.* **425,** 560–582
40. Prusky, G. T., Alam, N. M., Beekman, S., and Douglas, R. M. (2004) Rapid quantification of adult and developing mouse spatial vision using a virtual optomotor system. *Invest. Ophthalmol. Vis. Sci.* **45,** 4611–4616
41. Koulen, P., Fletcher, E. L., Craven, S. E., Bredt, D. S., and Wassle, H. (1998) Immunocytochemical localization of the postsynaptic density protein PSD-95 in the mammalian retina. *J. Neurosci.* **18,** 10136–10149
42. Imanishi, Y., Batten, M. L., Piston, D. W., Baehr, W., and Palczewski, K. (2004) Noninvasive two-photon imaging reveals retinyl ester storage structures in the eye. *J. Cell Biol.* **164,** 373–383
43. Noy, N. (2000) Retinoid-binding proteins: mediators of retinoid action. *Biochem. J.* **348**(Pt. 3), 481–495
44. Gupta, A., Williams, B. R., Hanash, S. M., and Rawwas, J. (2006) Cellular retinoic acid-binding protein II is a direct transcriptional target of MycN in neuroblastoma. *Cancer Res.* **66,** 8100–8108
45. Bastie, J. N., Despouy, G., Balitrand, N., Rochette-Egly, C., Chomienne, C., and Delva, L. (2001) The novel co-activator CRABPII binds to RARalpha and RXRalpha via two nuclear receptor interacting domains and does not require the AF-2 'core'. *FEBS Lett.* **507,** 67–73
46. Durand, B., Saunders, M., Leroy, P., Leid, M., and Chambon, P. (1992) All-trans and 9-cis retinoic acid induction of CRABPII transcription is mediated by RAR-RXR heterodimers bound to DR1 and DR2 repeated motifs. *Cell* **71,** 73–85
47. Berry, D. C., Soltanian, H., and Noy, N. (2010) Repression of cellular retinoic acid-binding protein II during adipocyte differentiation. *J. Biol. Chem.* **285,** 15324–15332
48. Kikonyogo, A., Abriola, D. P., Dryjanski, M., and Pietruszko, R. (1999) Mechanism of inhibition of aldehyde dehydrogenase by citral, a retinoid antagonist. *Eur. J. Biochem.* **262,** 704–712
49. Chrispell, J. D., Feathers, K. L., Kane, M. A., Kim, C. Y., Brooks, M., Khanna, R., Kurth, I., Hubner, C. A., Gal, A., Mears, A. J., Swaroop, A., Napoli, J. L., Sparrow, J. R., and Thompson, D. A. (2009) Rdh12 activity and effects on retinoid processing in the murine retina. *J. Biol. Chem.* **284,** 21468–21477
50. Liu, L. O., Li, G., McCall, M. A., and Cooper, N. G. (2000) Photoreceptor regulated expression of Ca(2+)/calmodulin-dependent protein kinase II in the mouse retina. *Brain Res. Mol. Brain Res.* **82,** 150–166
51. Si, J., Mueller, L., and Collins, S. J. (2007) CaMKII regulates retinoic acid receptor transcriptional activity and the differentiation of myeloid leukemia cells. *J. Clin. Invest.* **117,** 1412–1421
52. Nahoum, V., Perez, E., Germain, P., Rodriguez-Barrios, F., Manzo, F., Kammerer, S., Lemaire, G., Hirsch, O., Royer, C. A., Gronemeyer, H., de Lera, A. R., and Bourguet, W. (2007) Modulators of the structural dynamics of the retinoid X receptor to reveal receptor function. *Proc. Natl. Acad. Sci. U. S. A.* **104,** 17323–17328

53. Cvekl, A., and Wang, W. L. (2009) Retinoic acid signaling in mammalian eye development. *Exp. Eye Res.* **89,** 280–291
54. Duncan, T., Swint, C., Smith, S. B., and Wiggert, B. N. (1999) Levels of retinoic acid and retinaldehyde dehydrogenase expression in eyes of the Mitf-vit mouse model of retinal degeneration. *Mol. Vis.* **5,** 9
55. Weiler, R., Schultz, K., Pottek, M., Tieding, S., and Janssen-Bienhold, U. (1998) Retinoic acid has light-adaptive effects on horizontal cells in the retina. *Proc. Natl. Acad. Sci. U. S. A.* **95,** 7139–7144
56. Dmetrichuk, J. M., Spencer, G. E., and Carlone, R. L. (2005) Retinoic acid-dependent attraction of adult spinal cord axons towards regenerating newt limb blastemas in vitro. *Dev. Biol.* **281,** 112–120
57. Liu, S., Lau, L., Wei, J., Zhu, D., Zou, S., Sun, H. S., Fu, Y., Liu, F., and Lu, Y. (2004) Expression of Ca(2+)-permeable AMPA receptor channels primes cell death in transient forebrain ischemia. *Neuron* **43,** 43–55
58. Hollmann, M., Hartley, M., and Heinemann, S. (1991) Ca2+ permeability of KA-AMPA–gated glutamate receptor channels depends on subunit composition. *Science* **252,** 851–853
59. Mattson, M. P. (2008) Glutamate and neurotrophic factors in neuronal plasticity and disease. *Ann. N. Y. Acad. Sci.* **1144,** 97–112
60. Rongo, C., and Kaplan, J. M. (1999) CaMKII regulates the density of central glutamatergic synapses in vivo. *Nature* **402,** 195–199
61. De Koninck, P., and Schulman, H. (1998) Sensitivity of CaM kinase II to the frequency of Ca2+ oscillations. *Science* **279,** 227–230
62. Thiagarajan, T. C., Piedras-Renteria, E. S., and Tsien, R. W. (2002) alpha- and betaCaMKII. Inverse regulation by neuronal activity and opposing effects on synaptic strength. *Neuron* **36,** 1103–1114
63. Fink, C. C., Bayer, K. U., Myers, J. W., Ferrell, J. E., Jr., Schulman, H., and Meyer, T. (2003) Selective regulation of neurite extension and synapse formation by the beta but not the alpha isoform of CaMKII. *Neuron* **39,** 283–297
64. Solomin, L., Johansson, C. B., Zetterstrom, R. H., Bissonnette, R. P., Heyman, R. A., Olson, L., Lendahl, U., Frisen, J., and Perlmann, T. (1998) Retinoid-X receptor signalling in the developing spinal cord. *Nature* **395,** 398–402
65. Zhang, X. K., Lehmann, J., Hoffmann, B., Dawson, M. I., Cameron, J., Graupner, G., Hermann, T., Tran, P., and Pfahl, M. (1992) Homodimer formation of retinoid X receptor induced by 9-cis retinoic acid. *Nature* **358,** 587–591
66. Weiler, R., Schultz, K., and Janssen-Bienhold, U. (1995) Retraction of spinule-type neurites from carp retinal horizontal cell dendrites during dark adaptation involves the activation of Ca2+/calmodulin-dependent protein kinase II. *Eur. J. Neurosci.* **7,** 1914–1919
67. Maeda, A., Maeda, T., Golczak, M., Chou, S., Desai, A., Hoppel, C. L., Matsuyama, S., and Palczewski, K. (2009) Involvement of all-trans-retinal in acute light-induced retinopathy of mice. *J. Biol. Chem.* **284,** 15173–15183
68. Applebury, M. L., Antoch, M. P., Baxter, L. C., Chun, L. L., Falk, J. D., Farhangfar, F., Kage, K., Krzystolik, M. G., Lyass, L. A., and Robbins, J. T. (2000) The murine cone photoreceptor: a single cone type expresses both S and M opsins with retinal spatial patterning. *Neuron* **27,** 513–523
69. Fotiadis, D., Liang, Y., Filipek, S., Saperstein, D. A., Engel, A., and Palczewski, K. (2003) Atomic-force microscopy: Rhodopsin dimers in native disc membranes. *Nature* **421,** 127–128
70. Norris, A. W., Cheng, L., Giguere, V., Rosenberger, M., and Li, E. (1994) Measurement of subnanomolar retinoic acid binding affinities for cellular retinoic acid binding proteins by fluorometric titration. *Biochim. Biophys. Acta* **1209,** 10–18
71. Marc, R. E. (2010) Injury and repair: retinal remodeling. In *Encyclopedia of the Eye, Vol. 2* (Besharse, J. C., Dartt, D. A., and Dana, R., eds) pp: 414–420, Elsevier, New York
72. Chader, G. J., Weiland, J., and Humayun, M. S. (2009) Artificial vision: needs, functioning, and testing of a retinal electronic prosthesis. *Prog. Brain Res.* **175,** 317–332
73. Tomita, H., Sugano, E., Isago, H., Hiroi, T., Wang, Z., Ohta, E., and Tamai, M. (2010) Channelrhodopsin-2 gene transduced into retinal ganglion cells restores functional vision in genetically blind rats. *Exp. Eye Res.* **90,** 429–436
74. Thyagarajan, S., van Wyk, M., Lehmann, K., Lowel, S., Feng, G., and Wassle, H. (2010) Visual function in mice with photoreceptor degeneration and transgenic expression of channelrhodopsin 2 in ganglion cells. *J. Neurosci.* **30,** 8745–8758
75. Horsager, A., Greenberg, R. J., and Fine, I. (2010) Spatiotemporal interactions in retinal prosthesis subjects. *Invest. Ophthalmol. Vis. Sci.* **51,** 1223–1233
76. Pan, F., Paul, D. L., Bloomfield, S. A., and Volgyi, B. (2010) Connexin36 is required for gap junctional coupling of most ganglion cell subtypes in the mouse retina. *J. Comp. Neurol.* **518,** 911–927
77. Margolis, D. J., Newkirk, G., Euler, T., and Detwiler, P. B. (2008) Functional stability of retinal ganglion cells after degeneration-induced changes in synaptic input. *J. Neurosci.* **28,** 6526–6536
78. Fujikado, T., Kamei, M., Sakaguchi, H., Kanda, H., Morimoto, T., Ikuno, Y., Nishida, K., Kishima, H., Maruo, T., Konoma, K., and Ozawa, M. (2011) Testing of semichronically implanted retinal prosthesis by suprachoroidal-transretinal stimulation in patients with retinitis pigmentosa. *Invest. Ophthalmol. Vis. Sci.* **52,** 4726–4733
79. Benav, H., Bartz-Schmidt, K. U., Besch, D., Bruckmann, A., Gekeler, F., Greppmaier, U., Harscher, A., Kibbel, S., Kusnyerik, A., Peters, T., Sachs, H., Stett, A., Stingl, K., Wilhelm, B., Wilke, R., Wrobel, W., and Zrenner, E. (2010) Restoration of useful vision up to letter recognition capabilities using subretinal microphotodiodes. *Conf. Proc. IEEE Eng. Med. Biol. Soc.* **2010,** 5919–5922
80. Yang, P. B., Seiler, M. J., Aramant, R. B., Yan, F., Mahoney, M. J., Kitzes, L. M., and Keirstead, H. S. (2010) Trophic factors GDNF and BDNF improve function of retinal sheet transplants. *Exp. Eye Res.* **91,** 727–738
81. Busskamp, V., Duebel, J., Balya, D., Fradot, M., Viney, T. J., Siegert, S., Groner, A. C., Cabuy, E., Forster, V., Seeliger, M., Biel, M., Humphries, P., Paques, M., Mohand-Said, S., Trono, D., Deisseroth, K., Sahel, J. A., Picaud, S., and Roska, B. (2010) Genetic reactivation of cone photoreceptors restores visual responses in retinitis pigmentosa. *Science* **329,** 413–417
82. Doroudchi, M. M., Greenberg, K. P., Liu, J., Silka, K. A., Boyden, E. S., Lockridge, J. A., Arman, A. C., Janani, R., Boye, S. E., Boye, S. L., Gordon, G. M., Matteo, B. C., Sampath, A. P., Hauswirth, W. W., and Horsager, A. (2011) Virally delivered channelrhodopsin-2 safely and effectively restores visual function in multiple mouse models of blindness. *Mol. Ther.* **19,** 1220–1229
83. Altucci, L., Leibowitz, M. D., Ogilvie, K. M., de Lera, A. R., and Gronemeyer, H. (2007) RAR and RXR modulation in cancer and metabolic disease. *Nat. Rev. Drug Discov.* **6,** 793–810
84. Beltowski, J. (2008) Liver X receptors (LXR) as therapeutic targets in dyslipidemia. *Cardiovasc. Ther.* **26,** 297–316

Received for publication July 27, 2011.
Accepted for publication September 1, 2011.